Supporting Information

A near-infrared fluorescence probe based on the ICT (Intramolecular Charge Transfer) mechanism for the detection of hydrogen peroxide in cells.

Han Zeng[a#], Yuanyuan Wu[a#], Shijun Chen[b], Haijie Wang[a], Yaping Wang[a], Mingchao Huang[a], Yiyi Li[a], Xioadong Ma[a], Shicong Hou[a*].

a: College of Science, China Agricultural University, Beijing 100193, P.R. China

b: School of Chemistry and Chemical Engineering, Hainan University, Haikou 570228, P.R. China

E-mail address: houshc@cau.edu.cn

#: Both authors contributed equally to this study.

Table of Contents

1. Fluorescent probes for H_2O_2

Probe	NIR	λ_{em} (nm)	LOD (μM)	Response time (min)	Reference
HCyB	NO	556	0.076	90	[1]
BC-OB	NO	495	0.47	30	[2]
N-Py-BO	NO	650	0.57	30	[3]
RhB-NIR	Yes	730	0.061	15	[4]
QX-B	Yes	772	0.17	6	[5]
IR-990	Yes	990	0.59	20	[6]
Indo-H_2O_2	NO	617	0.025	25	[7]
DCA-Bba	NO	685	2.157	5	[8]
JH	Yes	775	4.72	95	This work

Scheme S1. Comparison of other fluorescent probes with JH.

2. Supplementary methods

2.1 Reagents and instruments

Unless otherwise stated, all reagents used were commercially purchased and used without purification. Detection of the visible ultraviolet spectrum using the PerkinElmer Lambda 650S UV−Vis absorption spectra were detected using a PerkinElmer LS55 fluorescence spectrometer. ^{1}H NMR and ^{13}C NMR spectra were obtained using a Bruker AvanceAVII-500 MHz spectrometer. High-resolution mass spectra were obtained by high-resolution mass spectrometry on an Agilent ESI-Q-TOF mass spectrometer. All live cell and zebrafish images were obtained using a Nikon A1 confocal microscope.

Determination of detecting limits

The detecting limits (DL) were calculated according to Eq.

$$DL = 3\sigma/k$$

Where σ is the standard derivation of blank solution and k is the slope of calibration curve.

2.2 Preparation of ROS/RNS/RSS

(1) Superoxide (O_2^-) was generated from KO_2 with a saturated solution of KO_2 in DMSO.
(2) The source of NaClO was from NaClO solution that contains 5% available chlorine.
(2) Hydroxyl radical (•OH) was generated by Fenton reactions by mixing $FeSO_4$•$7H_2O$ with H_2O_2, and the concentration of •OH was estimated from the concentration of Fe^{2+}.
(3) Preparation of $ONOO^-$. To a vigorously stirred solution of $NaNO_2$ (0.6 M, 10 mL) and H_2O_2 (0.7 M, 10 mL) in deionized H_2O at 0^oC was added HCl (0.6 M, 10 mL), immediately followed by the rapid addition of NaOH (1.5 M, 20 mL). Excess hydrogen peroxide was removed by passing the solution through a short column of MnO_2. The concentration of $ONOO^-$ was determined by UV analysis with the extinction coefficient at 302 nm (ε = 1670 M^{-1} cm^{-1}).
(4) Other interfering ions are configured according to conventional methods

2.3 Detection of the quantum yield of fluorescence

In our system, the fluorescence quantum yields of JH were determined in PBS buffer (10 mM)/DMSO, v/v 1/1 at 25℃, using Methylene blue (Φ_f = 0.80 in DMSO) as standard. The quantum yield was calculated using the following equation:

$$\Phi_x = \Phi_s(A_sF_x / A_xF_s)$$

where, A_x and A_s are the absorbance of the sample and the reference, respectively, at the same excitation wavelength, F_x and F_s are the corresponding relative integrated fluorescence intensities. Absorbance of sample and reference at their respective excitation wavelengths was controlled to be lower than 0.05.

3. Supplementary schemes

Compound A-1were synthesized based on the reference [6].

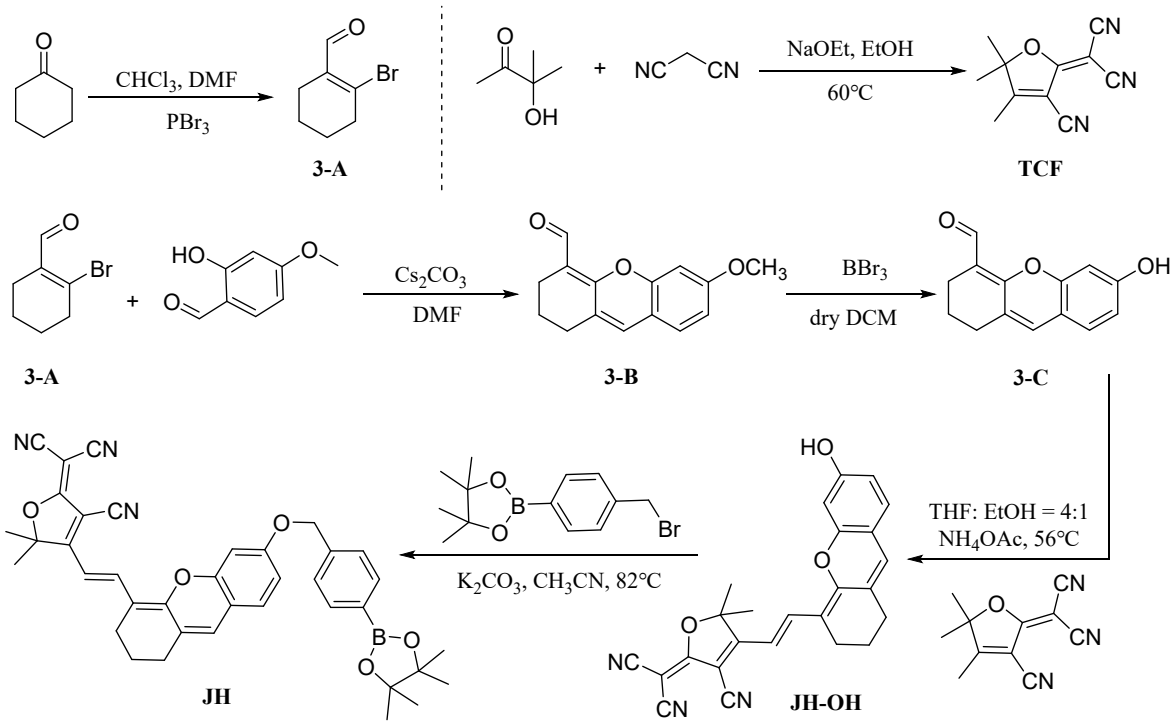

Scheme S2. Reaction scheme for probe and fluorophore synthesis.

Compound 3-B: The compounds 2-A (1.456 g, 7.70 mmol), 2-hydroxy-4-methoxybenzaldehyde (1.17 g, 7.70 mmol) and cesium carbonate (5.017 g, 15.4 mmol) were dissolved in 10 mL DMF under the protection of argon, and the reaction was stirred overnight at room temperature. After the reaction, the filter cake was washed with DCM and methanol, the filtrate was collected, after the removal of DCM and methanol by rotary evaporation, the reaction liquid was extracted with ethyl acetate, washed with water three times, the organic layer was dried and concentrated, and the column chromatography (PE: EA = 15:1-10:1) yellow solid compound 3-B was purified (0.537 g, 28.8% yield). 1H NMR (500 MHz, CDCl3) δ 10.29 (s, 1H), 7.06 (d, J = 8.4 Hz, 1H), 6.64 (d, J = 7.7 Hz, 3H), 3.82 (s, 3H), 2.59 - 2.50 (m, 2H), 2.42 (t, J = 5.9 Hz, 2H), 1.74 - 1.64 (m, 2H) ◦ 13C NMR (126 MHz, CDCl3) δ 187.59, 161.37, 160.78, 153.37, 127.46, 126.87, 126.57, 114.67, 112.55, 110.85, 100.48, 55.66, 29.93, 21.52,

20.40.

Compound 3-C: At 0℃, the anhydrous DCM solution of BBr3 (1.91 g, 7.64 mmol) was added to the anhydrous DCM solution of 4-3B (0.37 g, 1.53 mmol), and the reaction solution was heated at 0℃ for 1 h and then continued to react at room temperature for 16 h. After the reaction, the saturated NaHCO3 solution was added in the ice bath to quench the reaction, and then the reaction solution was extracted by DCM for three times, dried by anhydrous NaSO4, and the yellow-green solid compound 3-C was concentrated (0.29 g, 83.3% yield). 1H NMR (500 MHz, DMSO) δ 10.26 (d, J = 7.4 Hz, 2H), 7.25 (d, J = 8.3 Hz, 1H), 6.98 (s, 1H), 6.71 - 6.62 (m, 2H), 2.62 - 2.57 (m, 2H), 2.34 (t, J = 5.7 Hz, 2H), 1.72 - 1.60 (m, 2H) ◦ 13C NMR (126 MHz, DMSO) δ 186.61, 160.80, 160.18, 153.22, 128.62, 128.11, 125.19, 113.52, 112.48, 111.77, 102.34, 29.42, 21.70, 20.48.

Compound JH-OH: Under the protection of argon, 3-C (0.229 g, 1.0 mmol), TCF (0.199 g, 1.0 mmol) and ammonium acetate (0.085 g, 1.1 mmol) were dissolved in tetrahydrofuran and ethanol (THF: EtOH = 4:1) in 15 mL mixture, reflux reaction at 56℃ for 24 h. After the reaction liquid is cooled to room temperature, the filter is pumped, the filter cake is washed with DCM, and the solid material is collected to obtain the crude product. Then the blue-green compound JH-OH was purified by column chromatography (0.095 g, yield 23.2%).1H NMR (500 MHz, DMSO) δ 10.73 (s, 1H), 8.86 (d, J = 14.3 Hz, 1H), 7.43 - 7.38 (m, 2H), 6.76 (dd, J = 6.7, 2.3 Hz, 2H), 6.20 (d, J = 14.9 Hz, 1H), 2.70 - 2.64 (m, 2H), 2.55 (t, J = 5.9 Hz, 2H), 1.81 - 1.74 (m, 2H), 1.64 (s, 6H) ◦ 13C NMR (126 MHz, DMSO) δ 177.81, 161.71, 159.96, 154.17, 141.65, 133.25, 129.06, 125.88, 114.50, 114.38, 114.23, 113.78, 113.35, 107.67, 101.68, 97.34, 54.91, 39.52, 28.25, 25.61, 23.38, 20.04 ◦ HRMS Calcd for C25H19N3O3 [M+H]+ 410.1500,

found 410.1502.

Compound JH: The compounds JH-OH (0.067 g, 0.16 mmol) and K2CO3 (0.066 g, 0.48 mmol) were dissolved in 4 mL acetonitrile, stirred at room temperature for 15 min, and then added Pinalol 4-bromomethyl phenylborate (0.057 g, 0.192 mmol). The reaction was continued with reflux agitation at 82℃ for 4 h. After the reaction, the blue solid compound JH (0.025g, 25% yield) was purified by column chromatography (PE: EA = 5:1-2:1) after filtration, solids were removed, filtrate was collected and solvents were removed. 1H NMR (500 MHz, CDCl3) δ 8.62 (d, J = 13.7 Hz, 1H), 7.84 (d, J = 7.9 Hz, 2H), 7.45 (d, J = 7.8 Hz, 2H), 7.17 (d, J = 8.5 Hz, 1H), 6.87 (d, J = 17.1 Hz, 2H), 6.81 (dd, J = 8.5, 2.3 Hz, 1H), 6.05 (d, J = 15.3 Hz, 1H), 5.14 (s, 2H), 2.68 - 2.61 (m, 2H), 2.52 (t, J = 5.9 Hz, 2H), 1.89 - 1.83 (m, 2H), 1.69 (s, 6H), 1.34 (s, 12H) ◦ 13C NMR (126 MHz, CDCl3) δ 175.94, 172.45, 160.53, 157.86, 153.28, 141.07, 137.82, 134.13, 129.36, 126.81, 126.06, 125.79, 114.46, 112.41, 112.34, 111.91, 111.51, 107.23, 100.66, 95.27, 82.89, 69.49, 52.02, 30.41, 28.68, 28.64, 28.22, 25.75, 23.85, 22.92, 21.67, 19.45, 13.10.

4. Study on spectral properties

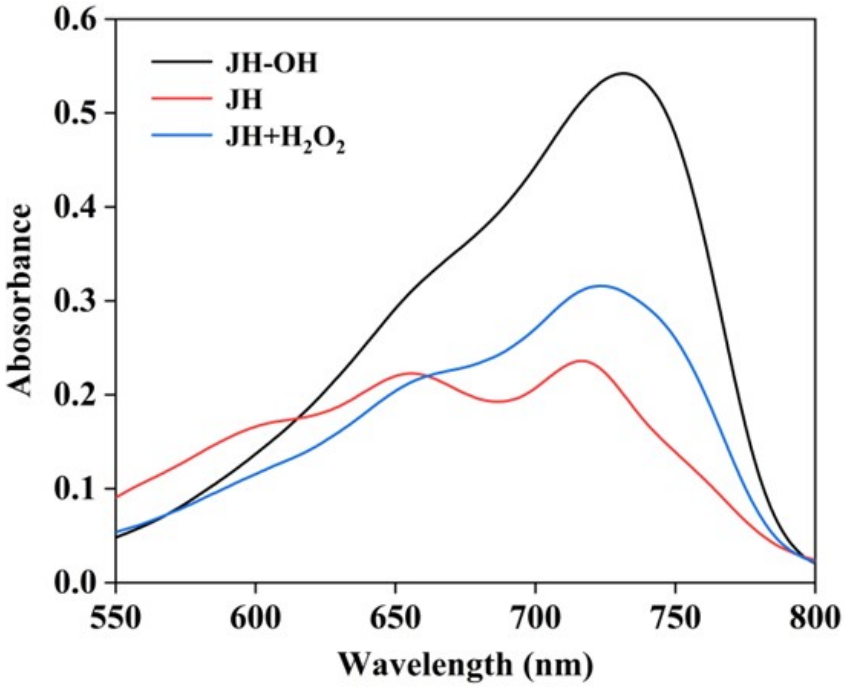

Fig. S1. Ultraviolet absorption spectra of probe JH (10 μM) and fluorophore JH-OH with and without H_2O_2 (1 mM). (PBS buffer 10.0 mM, pH 7.4).

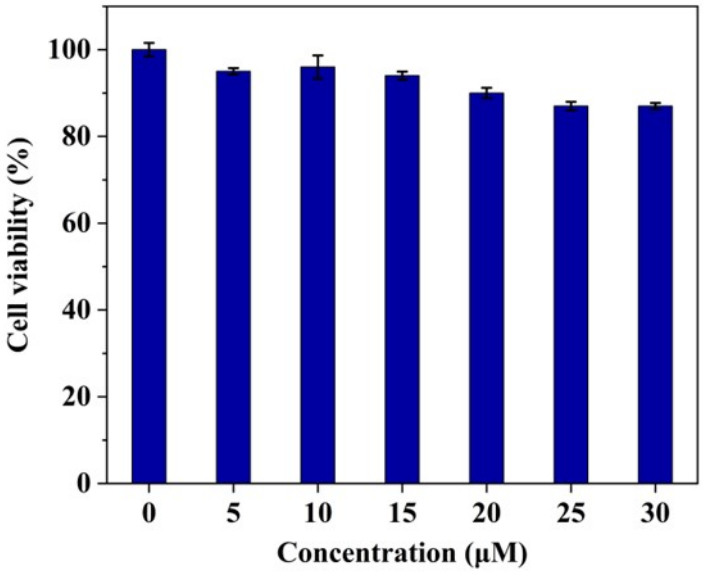

Fig. S2. MTT assay for the survival rate of HeLa cells treated with various concentrations of LTA (from 0 to 30 μM) for 24 h. Error bars represent the standard deviation (n = 3).

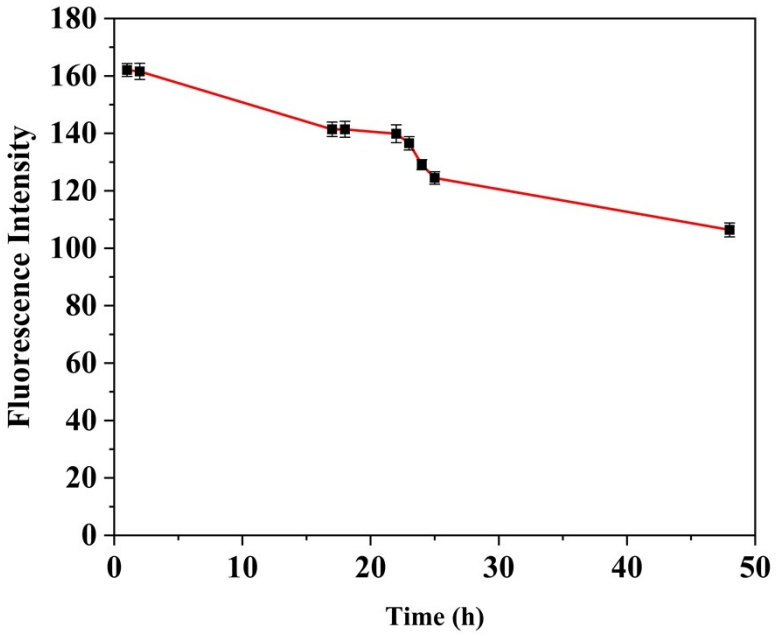

Fig. S3. Stability of probe JH over 48 hours.

5. ^{1}H-NMR, ^{13}C-NMR and HRMS analyses

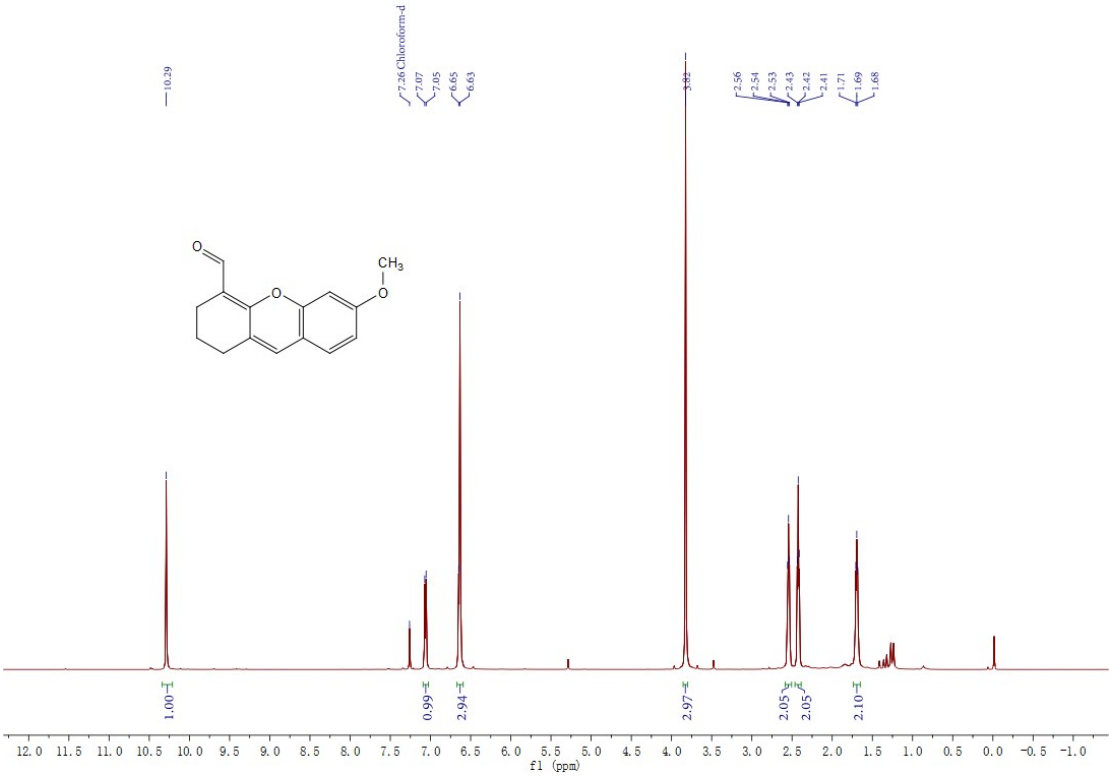

Fig. S4. ^{1}H NMR spectrum of 3-B

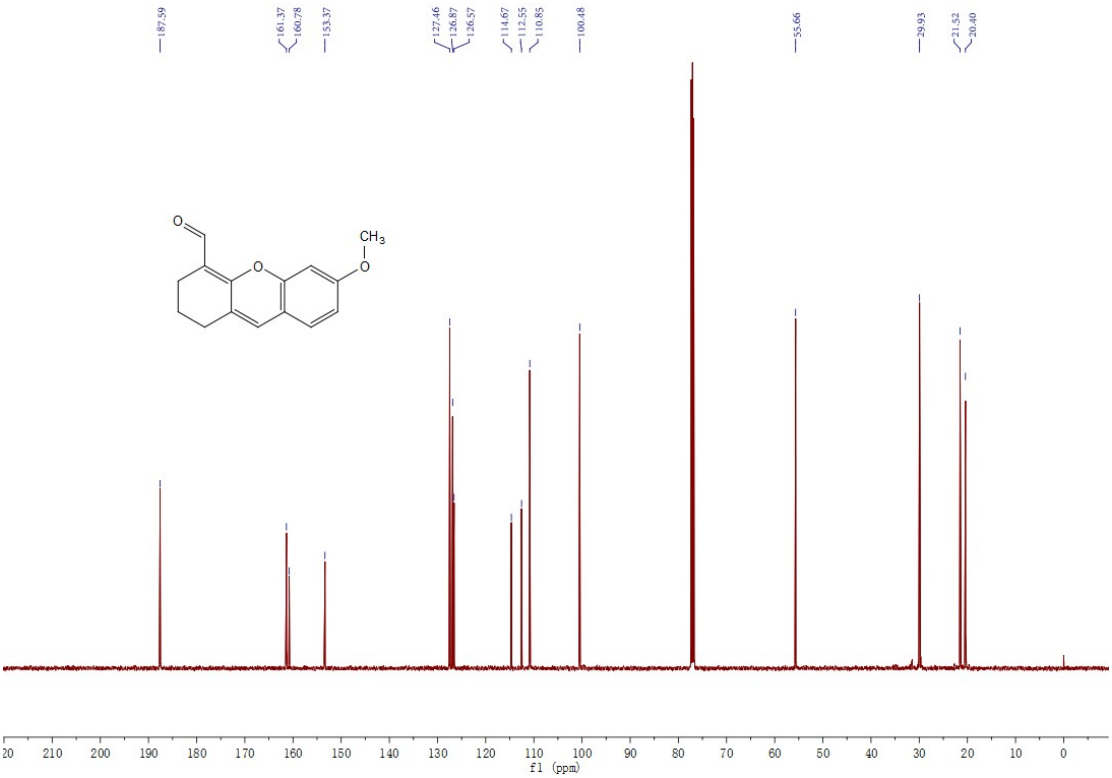

Fig. S5. ^{13}C NMR spectrum of 3-B

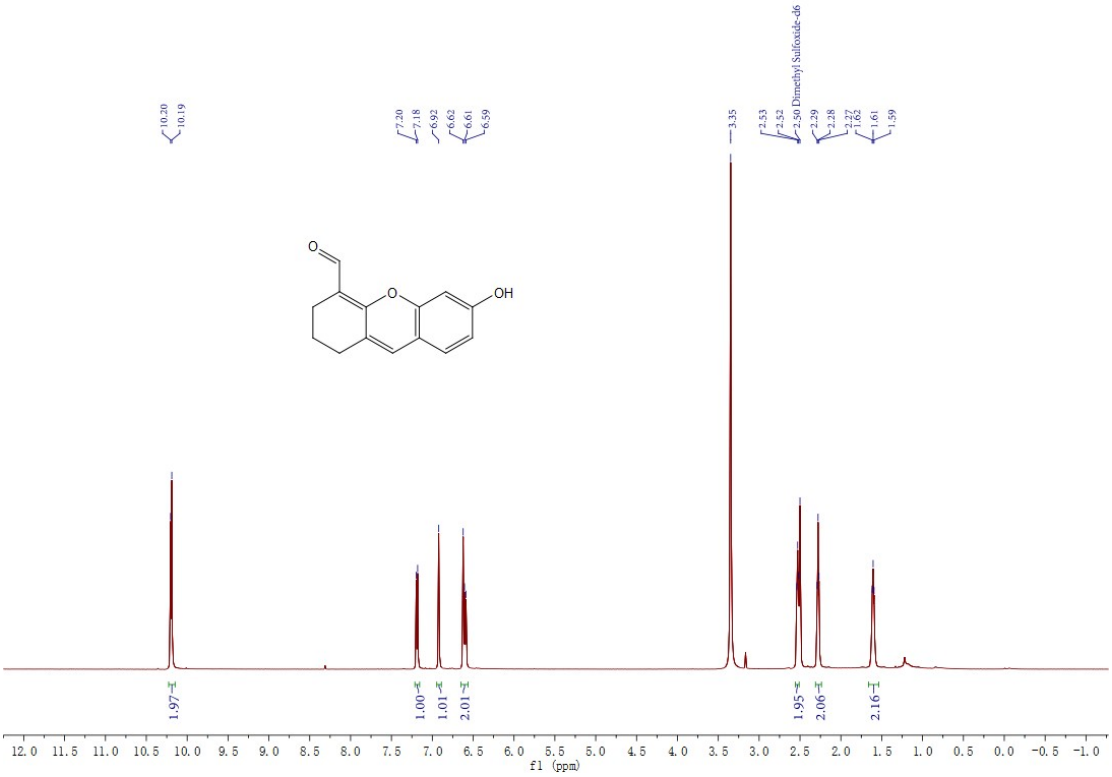

Fig. S6. ^{1}H NMR spectrum of 3-C

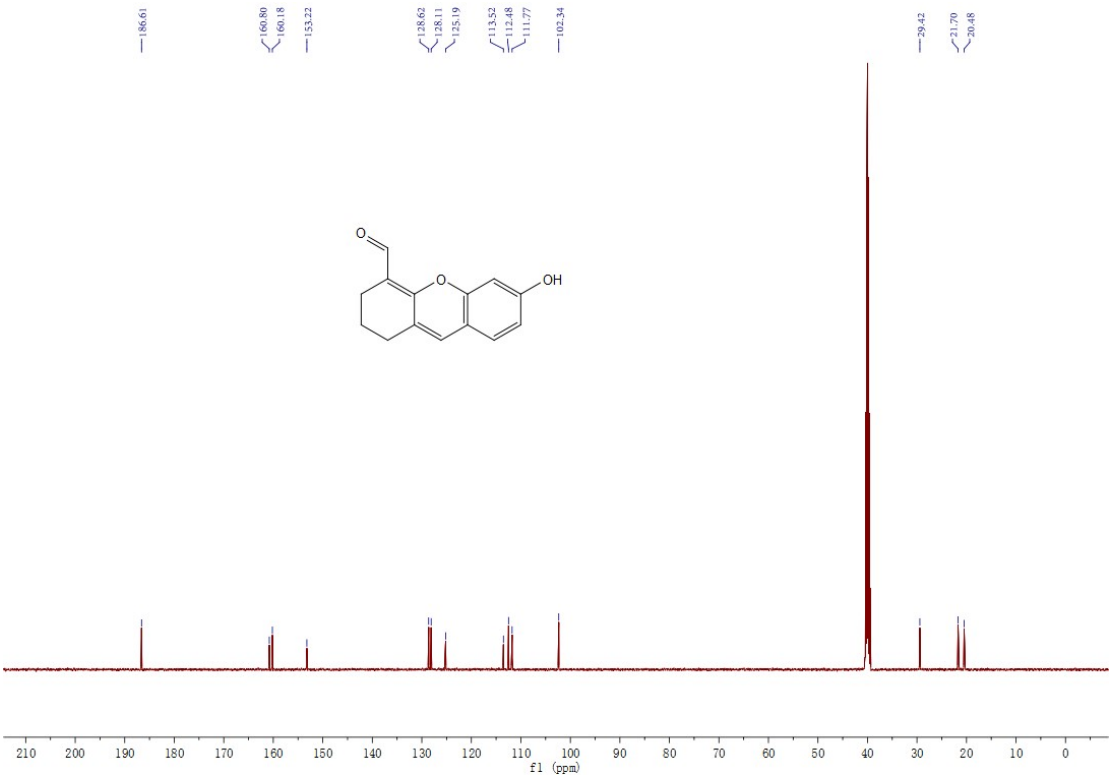

Fig. S7. ^{13}C NMR spectrum of 3-C

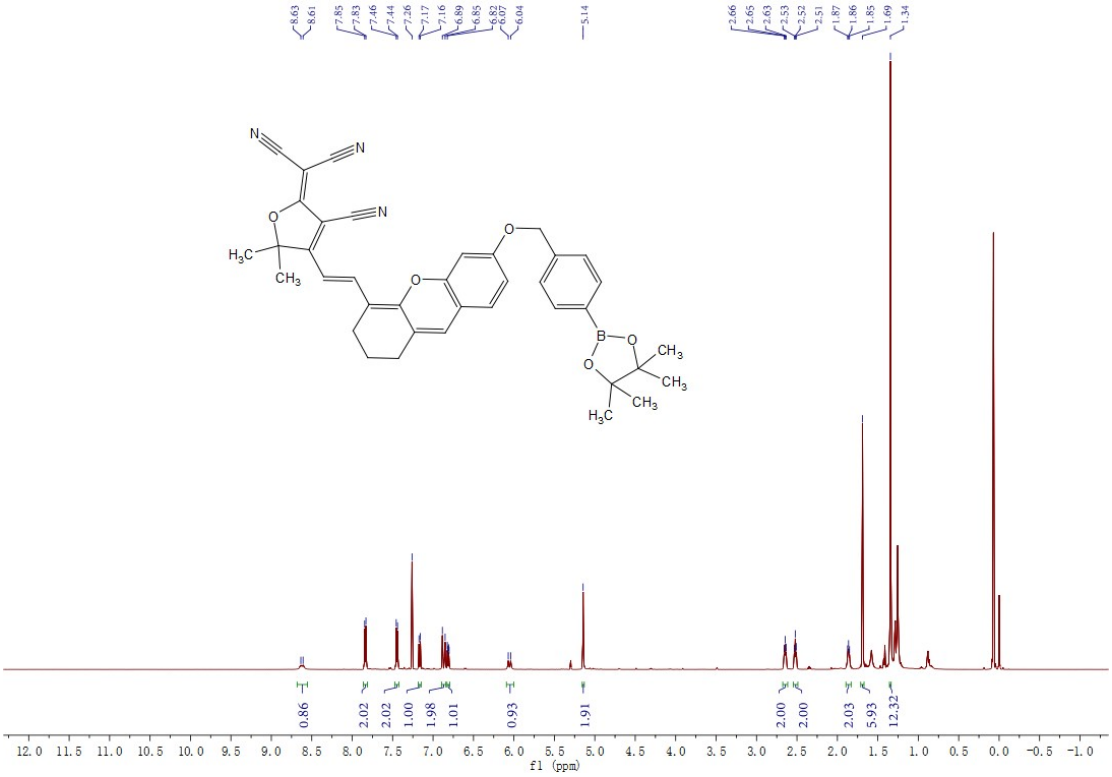

Fig. S8. ^{1}H NMR spectrum of JH

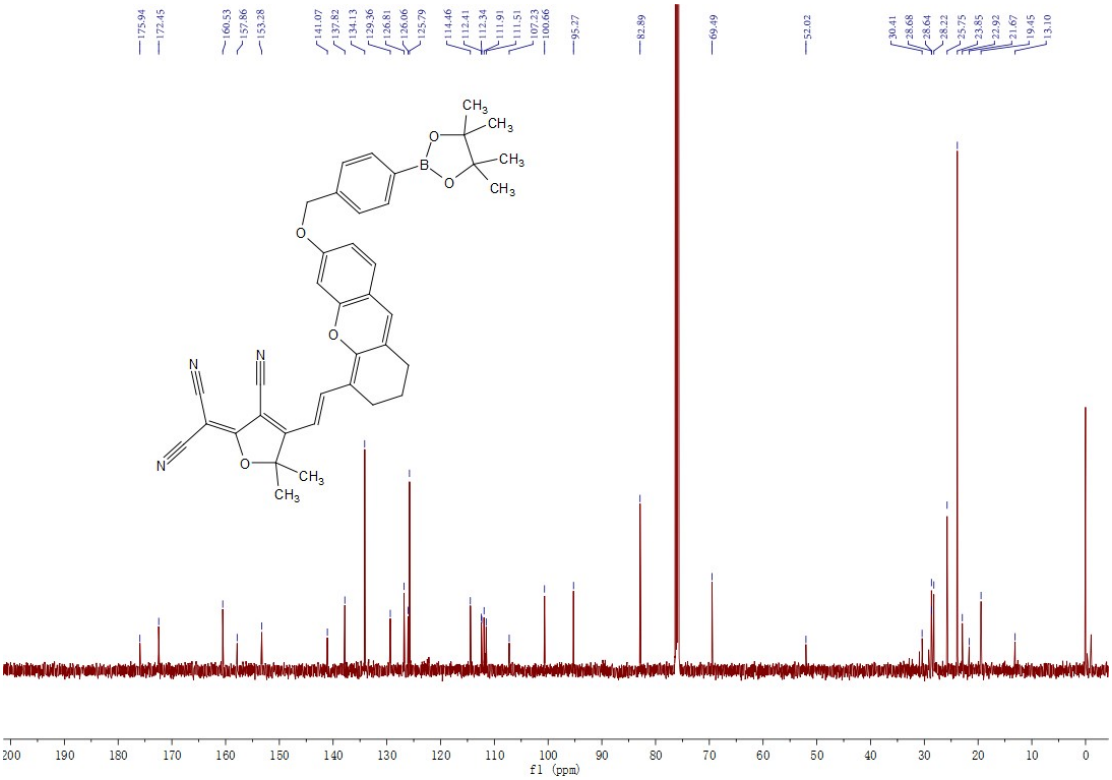

Fig. S9. ^{13}C NMR spectrum of JH

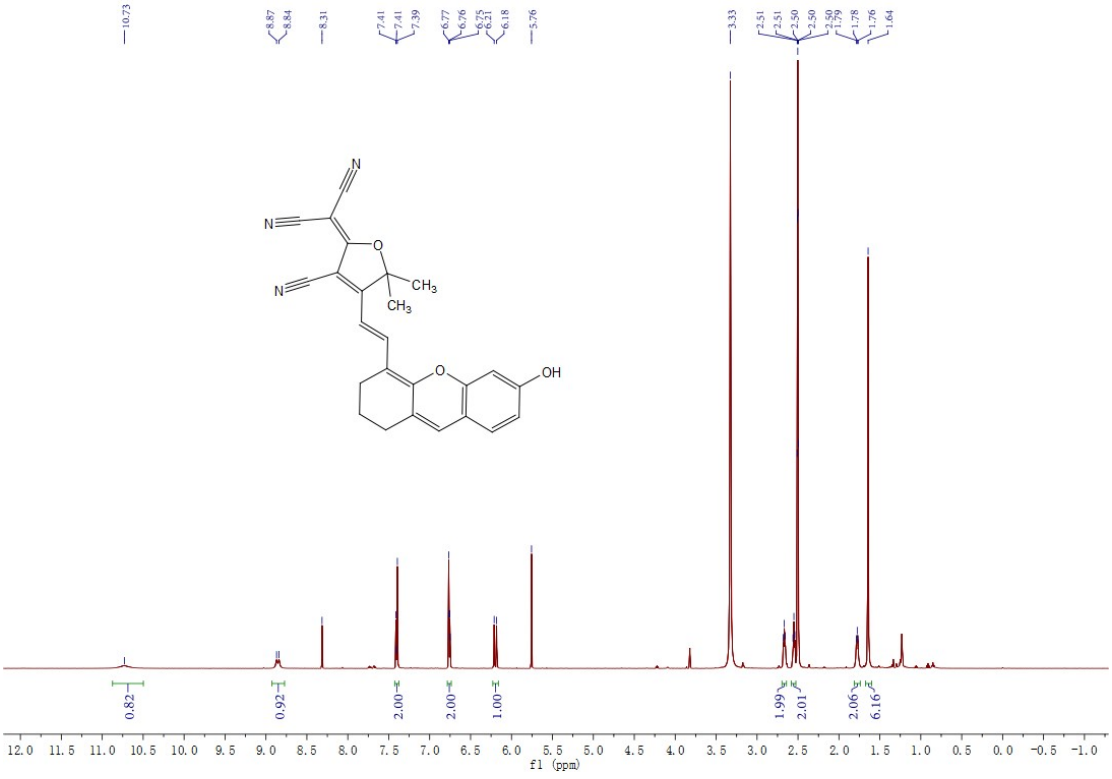

Fig. S10. ^{1}H NMR spectrum of JH-OH

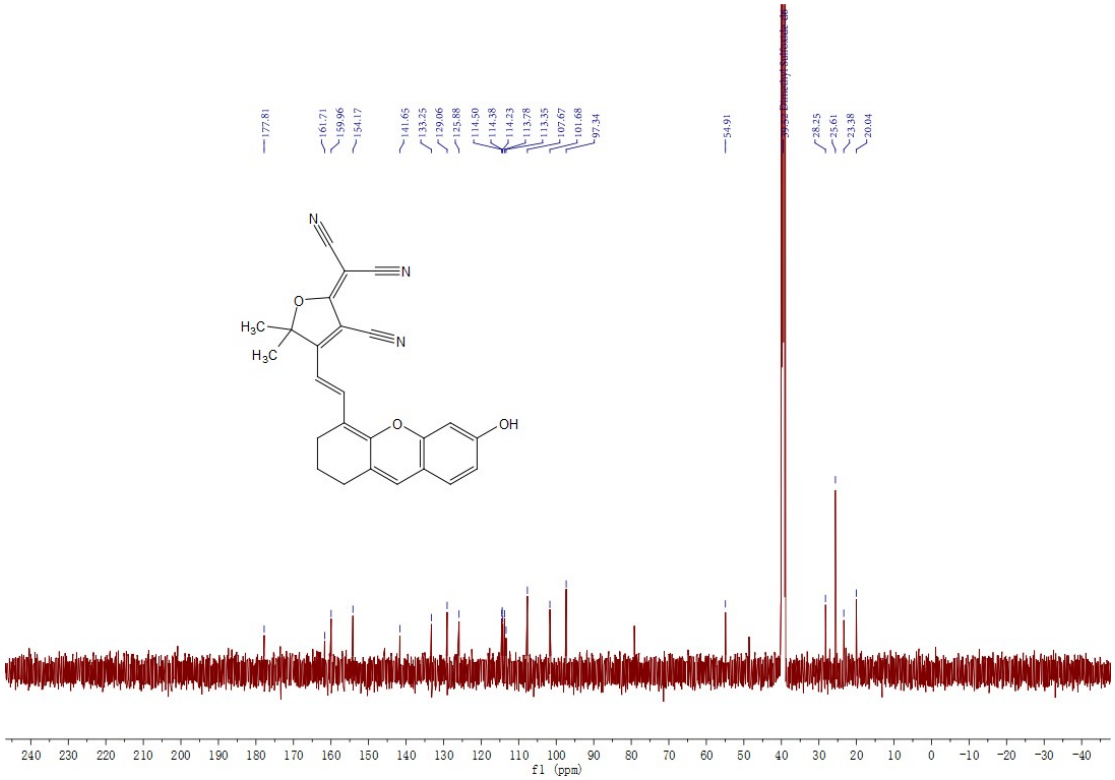

Fig. S11. ^{13}C NMR spectrum of JH-OH

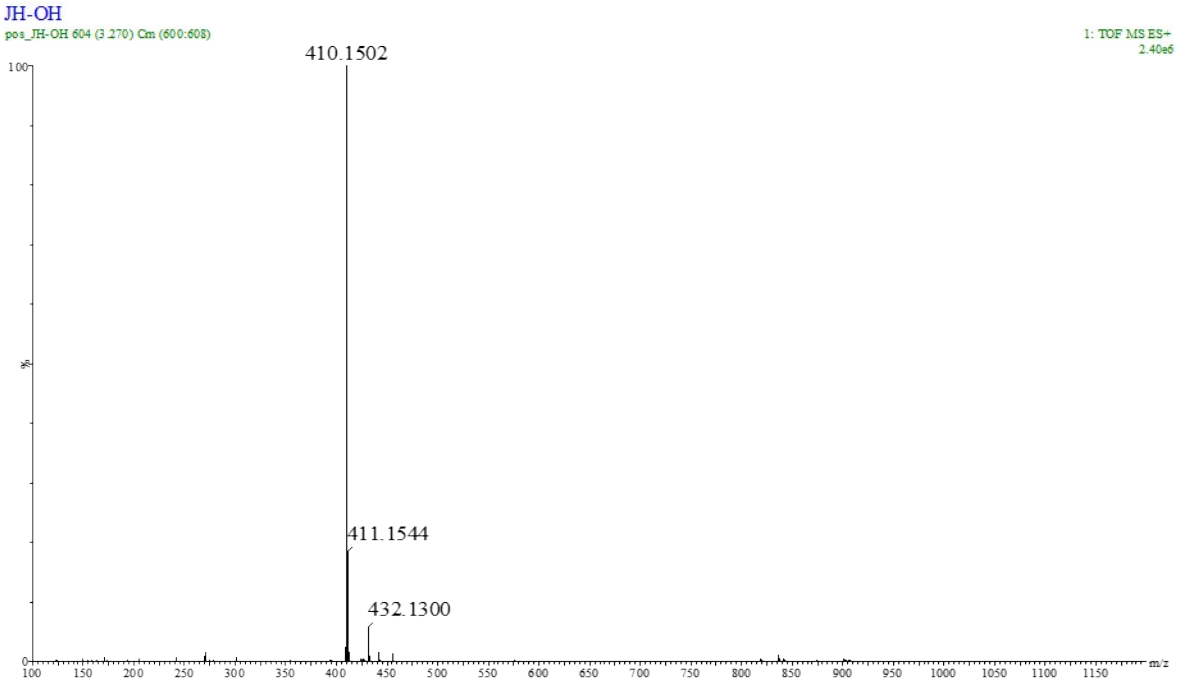

Fig. S12. High Resolution Mass Spectrogram of fluorophore JH-OH

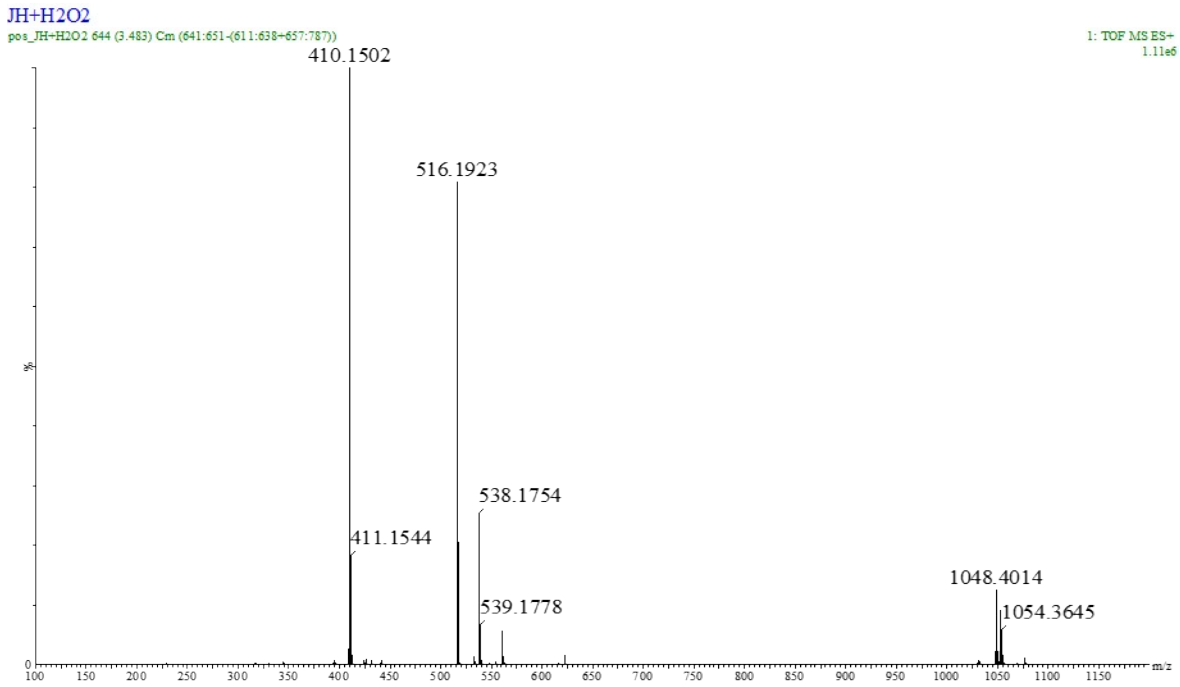

Fig. S13. High Resolution Mass Spectrogram of JH-OH reacted with H_2O_2

6. Reference

[1] J.J. Ciou, T.C. Wu, Z.J. Chen, B.L. Cheng, C.H. Lai, A selective fluorescent turn-on probe for imaging and sensing of hydrogen peroxide in living cells, Analytical and Bioanalytical Chemistry, 415 (2023) 4949-4959.

[2] Y.B. Wang, H.Z. Luo, C.Y. Wang, Z.Q. Guo, W.H. Zhu, A turn-on fluorescent probe based on π-extended coumarin for imaging endogenous hydrogen peroxide in RAW 264.7 cells, Journal of Photochemistry and Photobiology a-Chemistry, 414 (2021).

[3] J. Lu, L. Ji, Y.Y. Yu, Rational design of a selective and sensitive "turn-on" fluorescent probe for monitoring and imaging hydrogen peroxide in living cells, Rsc Advances, 11 (2021) 35093-35098.

[4] T. Gu, S. Mo, Y. Mu, X. Huang, L. Hu, Detection of endogenous hydrogen peroxide in living cells with para-nitrophenyl oxoacetyl rhodamine as turn-on mitochondria-targeted fluorescent probe, Sensors and Actuators B: Chemical, 309 (2020) 127731.

[5] W.-X. Wang, W.-L. Jiang, G.-J. Mao, M. Tan, J. Fei, Y. Li, C.-Y. Li, Monitoring the Fluctuation of Hydrogen Peroxide in Diabetes and Its Complications with a Novel Near-Infrared Fluorescent Probe, Analytical Chemistry, 93 (2021) 3301-3307.

[6] Y. Tian, S. Liu, W. Cao, P. Wu, Z. Chen, H. Xiong, H2O2-Activated NIR-II Fluorescent Probe with a Large Stokes Shift for High-Contrast Imaging in Drug-Induced Liver Injury Mice, Analytical Chemistry, 94 (2022) 11321-11328.

[7] N. Jain, P.M. Sonawane, A. Roychaudhury, S.J. Park, J. An, C.-H. Kim, S.B. Nimse, D.G. Churchill, An indole–based near–infrared fluorescent “Turn–On” probe for H2O2: Selective detection and ultrasensitive imaging of zebrafish gallbladder, Talanta, 269 (2024) 125459.

[8] L. Tian, X. Sun, L. Zhou, K. Zhong, S. Li, X. Yan, L. Tang, Reversible colorimetric and NIR fluorescent probe for sensing SO2/H2O2 in living cells and food samples, Food Chemistry, 407 (2023) 135031.